

# TOPOLOGICAL DERIVATIVES OF SHAPE FUNCTIONALS. PART 2

## FIRST ORDER METHOD AND APPLICATIONS

A.A. NOVOTNY, J. SOKOŁOWSKI, AND A. ŻOCHOWSKI

**ABSTRACT.** The framework of topological sensitivity analysis in singularly perturbed geometrical domains, presented in the first part of this series of review papers, allows for the asymptotic expansion of a given shape functional with respect to a small parameter that measures the size of singular domain perturbations, such as holes, cavities, inclusions, source-terms and cracks. This new concept in shape sensitivity analysis generalizes the shape derivatives from the domain boundary to its interior for admissible domains in two and three spatial dimensions. Therefore, the concept of topological derivative is a powerful tool for the solution of shape-topology optimization problems. There are now applications of the topological derivative method in many different fields of engineering and physics such as shape and topology optimization in structural mechanics, inverse problems for partial differential equations, imaging processing, multi-scale material design and mechanical modeling including damage and fracture evolution phenomena. In this second part of review the topology optimization algorithm based on the first order topological derivative is presented. The appropriate level-set domain representation method is employed within the iterations in order to design an optimal shape-topology local solution. The algorithm is successfully used for numerical solution of a wide class of shape-topology optimization problems.

### 1. INTRODUCTION

The topological derivative, presented in the first part of this series of review papers (Part 1), represents the first term of the asymptotic expansion of a given shape functional with respect to the small parameter which measures the size of singular domain perturbations, such as holes, inclusions, source-terms and cracks. This relatively new concept has been successfully applied to many relevant fields such as shape and topology optimization, inverse problems, imaging processing, multiscale material design and mechanical modeling including damage and fracture evolution phenomena.

It is worth to mention that the topological derivative is defined through a limit passage when the small parameter governing the size of the topological perturbation goes to zero. Therefore, it can be used as a steepest-descent direction in an optimization process like in any method based on the gradient of the cost functional. In particular, in this second part of review papers on the topological derivative concept, a topology optimization algorithm based on the first order topological derivative together with a level-set domain representation method is presented [13]. Finally, these ideas are used for solving a wide class of a topology optimization problems.

In order to introduce these ideas, let us consider an open and bounded domain  $\Omega \subset \mathbb{R}^d$ ,  $d \geq 2$ , with Lipschitz continuous boundary  $\partial\Omega$ . The domain  $\Omega$  is subjected to a perturbation confined in a small arbitrary-shaped set  $\omega_\varepsilon(\hat{x})$  of size  $\varepsilon$  and center at an arbitrary point  $\hat{x}$  of  $\Omega$ , such that  $\overline{\omega_\varepsilon(\hat{x})} \subset \Omega$ . We introduce a characteristic function  $x \mapsto \chi(x)$ ,  $x \in \mathbb{R}^d$ , associated to the unperturbed domain, namely  $\chi = \mathbf{1}_\Omega$ . Then, we define a characteristic function associated to the topologically perturbed domain of the form  $x \mapsto \chi_\varepsilon(\hat{x}; x)$ ,  $x \in \mathbb{R}^d$ . In the case of a hole, for example,  $\chi_\varepsilon(\hat{x}) = \mathbf{1}_\Omega - \mathbf{1}_{\overline{\omega_\varepsilon(\hat{x})}}$  and the perturbed domain is given by  $\Omega_\varepsilon(\hat{x}) = \Omega \setminus \overline{\omega_\varepsilon(\hat{x})}$ . Then, we assume that a given shape functional  $\psi(\chi_\varepsilon(\hat{x}))$ , associated to the topologically perturbed domain, admits the following topological asymptotic expansion [75]

$$\psi(\chi_\varepsilon(\hat{x})) = \psi(\chi) + f(\varepsilon)\mathcal{T}(\hat{x}) + o(f(\varepsilon)), \quad (1.1)$$

where  $\psi(\chi)$  is the shape functional associated to the unperturbed domain and  $f(\varepsilon)$  is a positive function such that  $f(\varepsilon) \rightarrow 0$  when  $\varepsilon \rightarrow 0$ . The function  $\hat{x} \mapsto \mathcal{T}(\hat{x})$  is called the topological derivative of  $\psi$  at  $\hat{x}$ . Therefore, the term  $f(\varepsilon)\mathcal{T}(\hat{x})$  represents a first order correction of  $\psi(\chi)$  to approximate  $\psi(\chi_\varepsilon(\hat{x}))$ .

In contrast to the nucleation of holes as discussed in Part 1, the domain can also be topologically perturbed by the nucleation of a small inclusion. It allows for working in a fixed computational domain  $\mathcal{D} \subset \mathbb{R}^d$ , where a weak material phase is used to mimic voids. This simple strategy avoids the use of complicated algorithm specific designed to deal with nucleation of holes in a computational domain. Let us consider that the hold-all domain  $\mathcal{D}$  is split into two subdomains, namely,  $\Omega \subset \mathcal{D}$  and its complement  $\mathcal{D} \setminus \Omega$ . We assume that there is a distributed parameter  $\rho : \mathcal{D} \mapsto \{1, \rho_0\}$  defined as

$$\rho(x) := \begin{cases} 1, & \text{if } x \in \Omega, \\ \rho_0, & \text{if } x \in \mathcal{D} \setminus \Omega. \end{cases} \quad (1.2)$$

with  $0 < \rho_0 \ll 1$ . Let us introduce a shape functional  $\Omega \mapsto J(\Omega)$ . The topology optimization problem we are dealing with is stated as follows:

$$\text{Minimize}_{\Omega \subset \mathcal{D}} J(\Omega), \quad (1.3)$$

which can be solved by using the topological derivative concept. Actually, a hole  $\omega_\varepsilon(\hat{x})$  is introduced inside  $\mathcal{D}$ . Then, the region occupied by  $\omega_\varepsilon(\hat{x})$  is filled by an inclusion with different material property from the background. The material properties are characterized by a piecewise constant function  $\gamma_\varepsilon$  of the form

$$\gamma_\varepsilon(x) := \begin{cases} 1 & \text{if } x \in \mathcal{D} \setminus \overline{\omega_\varepsilon}, \\ \gamma(x) & \text{if } x \in \omega_\varepsilon, \end{cases} \quad (1.4)$$

where the contrast  $\gamma$  is defined as

$$\gamma(x) = \begin{cases} \rho_0, & \text{if } x \in \Omega, \\ \rho_0^{-1}, & \text{if } x \in \mathcal{D} \setminus \Omega, \end{cases} \quad (1.5)$$

which induces a level-set domain representation method. In fact, let us explain better these ideas in Section 2. The topology optimization problem we are dealing with is presented in Section 3, together with a wide class of applications. In particular, Section 3.1 deals with several structure topology optimization problems. In Section 3.2 a fluid flow channels design problem is presented. Section 3.3 is dedicated to the synthesis of materials in a multiscale framework. Some additional applications found in the current literature are discussed in Section 3.4. Finally, the paper ends with some concluding remarks and open problems in Section 4.

## 2. FIRST ORDER ALGORITHM

In this section a topology optimization algorithm based on the first order topological derivative together with a level-set domain representation method is presented. It has been proposed in [13] and consists basically in achieving a local optimality condition for the minimization problem (1.3), given in terms of the topological derivative and a level-set function. In particular, the domain  $\Omega \subset \mathcal{D}$  and the complement  $\mathcal{D} \setminus \Omega$  are characterized by a level-set function  $\Psi$  of the form:

$$\Omega = \{x \in \mathcal{D} : \Psi(x) < 0\} \quad \text{and} \quad \mathcal{D} \setminus \Omega = \{x \in \mathcal{D} : \Psi(x) > 0\}, \quad (2.1)$$

where  $\Psi$  vanishes on the interface between  $\Omega$  and  $\mathcal{D} \setminus \Omega$ . A local sufficient optimality condition for Problem (1.3), under a class of domain perturbation given by ball-shaped inclusions denoted by  $B_\varepsilon(x)$ , can be stated as [12]

$$\mathcal{T}(x) > 0 \quad \forall x \in \mathcal{D}, \quad (2.2)$$

where  $\mathcal{T}(x)$  is the topological derivative of the shape functional  $J(\Omega)$  at  $x \in \mathcal{D}$  and  $B_\varepsilon(x)$  is a ball of radius  $\varepsilon$  and center at  $x \in \mathcal{D}$ , as shown in the sketch of Fig. 1. Therefore, let us define

the quantity

$$g(x) := \begin{cases} -\mathcal{T}(x), & \text{if } \Psi(x) < 0, \\ +\mathcal{T}(x), & \text{if } \Psi(x) > 0, \end{cases} \quad (2.3)$$

which allows for rewriting the condition (2.2) in the following equivalent form

$$\begin{cases} g(x) < 0, & \text{if } \Psi(x) < 0, \\ g(x) > 0, & \text{if } \Psi(x) > 0. \end{cases} \quad (2.4)$$

We observe that (2.4) is satisfied wether the quantity  $g$  coincides with the level-set function  $\Psi$  up to a strictly positive number, namely  $\exists \tau > 0 : g = \tau\Psi$ , or equivalently

$$\theta := \arccos \left[ \frac{\langle g, \Psi \rangle_{L^2(\mathcal{D})}}{\|g\|_{L^2(\mathcal{D})} \|\Psi\|_{L^2(\mathcal{D})}} \right] = 0, \quad (2.5)$$

which shall be used as optimality condition in the topology design algorithm, where  $\theta$  is the angle between the functions  $g$  and  $\Psi$  in  $L^2(\mathcal{D})$ .

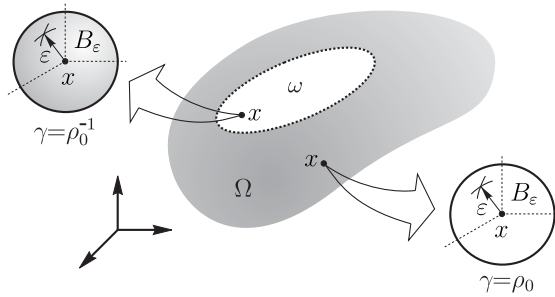


FIGURE 1. Nucleation of a ball-shaped inclusion  $B_\epsilon(x)$ .

Let us now explain the algorithm. We start by choosing an initial level-set function  $\Psi_0$ . In a generic iteration  $n$ , we compute the function  $g_n$  associated with the level-set function  $\Psi_n$ . Thus, the new level-set function  $\Psi_{n+1}$  is updated according to the following linear combination between the functions  $g_n$  and  $\Psi_n$

$$\begin{aligned} \Psi_0 : \|\Psi_0\|_{L^2(\mathcal{D})} &= 1, \\ \Psi_{n+1} &= \frac{1}{\sin \theta_n} \left[ \sin((1 - \kappa)\theta_n)\Psi_n + \sin(\kappa\theta_n) \frac{g_n}{\|g_n\|_{L^2(\mathcal{D})}} \right] \quad \forall n \in \mathbb{N}, \end{aligned} \quad (2.6)$$

where  $\theta_n$  is the angle between  $g_n$  and  $\Psi_n$ , and  $\kappa$  is a step size determined by a line-search performed in order to decrease the value of the objective function  $J(\Omega_n)$ , with  $\Omega_n$  used to denote the domain associated with  $\Psi_n$ . The process ends when the condition  $\theta_n \leq \epsilon_\theta$  is satisfied in some iteration, where  $\epsilon_\theta$  is a given small numerical tolerance. Since we have chose  $\Psi_0 : \|\Psi_0\|_{L^2(\mathcal{D})} = 1$ , then by construction  $\Psi_{n+1} : \|\Psi_{n+1}\|_{L^2(\mathcal{D})} = 1 \quad \forall n \in \mathbb{N}$ . If at some iteration  $n$  the line-search step size  $\kappa$  is found to be smaller than a given numerical tolerance  $\epsilon_\kappa > 0$  and the optimality condition is not satisfied, namely  $\theta_n > \epsilon_\theta$ , then a mesh refinement of the hold all domain  $\mathcal{D}$  is carried out and the iterative process is continued. The resulting first order topology design algorithm is summarized in a pseudo-code format shown in Algorithm 1. For further applications of this algorithm, see for instance [6, 17, 18, 19, 64, 65, 49, 80, 87].

In the context of topological derivative-based topology optimization methods, the algorithms available in the literature usually combine the topological derivative with shape derivative or level-set methods [2, 28, 38, 77], leading to a two-stage topology/shape optimization procedure. More precisely, new holes are nucleated according to the topological derivative, while standard tools in shape optimization are used to move the new boundaries. In contrast, Algorithm 1 is based on the optimality condition (2.2) written in terms of the topological derivative and a level-set function, leading to a very simple and quite efficient one-stage algorithm driven by the

---

**Algorithm 1:** The topology design algorithm
 

---

**input** :  $\mathcal{D}$ ,  $\Psi_0$ ,  $\epsilon_\kappa$ ,  $\epsilon_\theta$ ;  
**output**: the optimal topology  $\Omega^*$ ;  
**1**  $n \leftarrow 0$ ;  
**2**  $\Omega_n \leftarrow \Psi_n$ ;  
**3** compute the shape functional  $J(\Omega_n)$ ;  
**4** compute the associated topological derivative  $\mathcal{T}(x)$ ;  
**5** compute  $g_n$  and  $\theta_n$  according to (2.3) and (2.5);  
**6**  $\Psi_{\text{old}} \leftarrow \Psi_n$ ;  $J_{\text{old}} \leftarrow J(\Omega_n)$ ;  $J_{\text{new}} \leftarrow 1 + J_{\text{old}}$ ;  $\kappa \leftarrow 1$ ;  
**7** **while**  $J_{\text{new}} > J_{\text{old}}$  **do**  
**8**     compute  $\Psi_{\text{new}}$  according to (2.6);  
**9**      $\Psi_n \leftarrow \Psi_{\text{new}}$ ;  
**10**    execute lines 2 and 3;  
**11**     $J_{\text{new}} \leftarrow J(\Omega_n)$ ;  
**12**     $\kappa \leftarrow \kappa/2$ ;  
**13** **end while**  
**14** **if**  $\kappa < \epsilon_\kappa$  **then**  
**15**     try a mesh refinement;  
**16**      $\Psi_{n+1} \leftarrow \Psi_n$ ;  $n \leftarrow n + 1$ ;  
**17**     **go to** line 2;  
**18** **else if**  $\theta_n > \epsilon_\theta$  **then**  
**19**      $\Psi_{n+1} \leftarrow \Psi_n$ ;  $n \leftarrow n + 1$ ;  
**20**     **go to** line 2;  
**21** **else**  
**22**     **return**  $\Omega^* \leftarrow \Psi_n$ ;  
**23**     **stop**;  
**24** **end if**

---

topological derivative only. We claim however that how to efficiently use the topological derivative in the context of topology optimization is a field under development which still deserves further investigation. See Section 4 for an account on some open problems.

### 3. SHAPE AND TOPOLOGY OPTIMIZATION

The topological derivative has been specifically designed to deal with shape and topology optimization. It has been introduced by Sokołowski & Żochowski in the fundamental paper [84] to fill a gap in the existing literature at that time. Actually, the idea was to give a precise (mathematical) answer to the following question: What does happen when a hole is nucleated? The answer to this question is not trivial at all. In fact, when a hole is nucleated, singularities would appear. Therefore, in order to deal with this problem, the theory of asymptotic analysis in singularly perturbed geometrical domain is need. The difficulty in finding a convenient formula of the topological derivative for numerics purposes should be noted. It requires technical derivations strongly dependent on the problem under analysis, which may limit its range of real world applications. On the other hand, in contrast to traditional topology optimization methods, the topological derivative formulation does not require a material model concept based on intermediary densities, so that interpolation schemes are unnecessary. These features are crucial in a wide range of applications, since the limitations arising from material model procedures are here naturally avoided. In addition, topological derivative has the advantage of providing an analytical form for the topological sensitivity which allows to obtain the optimal design in a few iterations or even in just one shot. Therefore, the resulting topology optimization algorithms are remarkably efficient and of simple computational implementation, since it features only a

minimal number of user-defined algorithmic parameters. In this section, the first order topology design Algorithm 1 is applied in the context of shape and topology optimization. See also related works [2, 26, 28, 48, 58, 62, 72, 73, 74, 89].

**3.1. Structural Design.** This section deals with structural topology optimization problems [1, 25, 39, 75]. We start with two benchmark examples concerning structural compliance minimization under volume constraint, one of them into two and the other one into three spatial dimensions. The next two examples consist in the volume minimization under stress constraints in the context of structural optimization and design of compliant mechanisms, respectively. Finally, we present an example concerning structural topology optimization under loading uncertainties.

Let us introduce the hold-all domain  $\mathcal{D} \subset \mathbb{R}^d$ ,  $d \geq 2$ , with Lipschitz boundary  $\Gamma := \partial\mathcal{D}$ . The elasticity boundary value problem which we are dealing with is stated as follows: Find the displacement vector field  $u$ , such that

$$\begin{cases} -\operatorname{div}\sigma(u) = 0 & \text{in } \mathcal{D}, \\ \sigma(u) = \mathbb{C}(\nabla u)^s, & \\ u = 0 & \text{on } \Gamma_D, \\ \sigma(u)n = \bar{q} & \text{on } \Gamma_N. \end{cases} \quad (3.1)$$

In the above elasticity system,  $(\nabla u)^s$  is the symmetric part of the gradient of  $u$  and  $\mathbb{C}$  is the fourth order elasticity tensor, which can be written in terms of the Lamé's coefficients  $\mu$  and  $\lambda$  as follows

$$\mathbb{C} = 2\mu\mathbb{I} + \lambda(\mathbf{I} \otimes \mathbf{I}), \quad (3.2)$$

with  $\mathbf{I}$  and  $\mathbb{I}$  used to denote the second and fourth order identity tensors, respectively. In addition,  $\Gamma = \bar{\Gamma}_D \cup \bar{\Gamma}_N$  with  $\Gamma_D \cap \Gamma_N = \emptyset$ , where  $\Gamma_D$  and  $\Gamma_N$  are Dirichlet and Neumann boundaries, respectively. Thus  $\bar{q}$  is a Neumann data on  $\Gamma_N$ , assumed to be smooth enough. The strain energy stored in the elastic body is minimized under a volume constraint. Therefore, the topology optimization problem we are dealing with consists in finding a subdomain  $\Omega \subset \mathcal{D}$  that solves the following minimization problem:

$$\text{Minimize}_{\Omega \subset \mathcal{D}} \mathcal{F}_\Omega(u) = \mathcal{J}(u) + \beta|\Omega|, \quad (3.3)$$

where  $\beta$  is a fixed multiplier used to impose a volume constraint in  $\Omega$  of the form  $|\Omega| \leq M$  and  $\mathcal{J}(u)$  is the energy shape functional, that is

$$\mathcal{J}(u) = \frac{1}{2} \int_{\mathcal{D}} \sigma(u) \cdot (\nabla u)^s. \quad (3.4)$$

The vector function  $u$  is solution to the elasticity boundary value problem (3.1). In particular, by fixing different values of  $\beta$  we get different volume fractions at the end of the iterative process. For more sophisticated topological derivative-based methods dealing with volume constraint we refer the reader to [30], for instance.

Let us consider the elasticity boundary value problem into two spatial dimensions, namely  $\mathcal{D} \subset \mathbb{R}^2$ . The topological perturbation we are dealing with consists in the nucleation of a small circular inclusion  $\omega_\varepsilon(x) = B_\varepsilon(x)$  endowed with a contrast  $\gamma_\varepsilon$  according to (1.4). In this case, the associated topological derivative is given by the sum

$$\mathcal{T}(x) = \mathcal{T}_E(x) + \beta\mathcal{T}_V(x) \quad \forall x \in \Omega. \quad (3.5)$$

The last term  $\mathcal{T}_V(x)$  represents the topological derivative of the volume, which is trivially given by

$$\mathcal{T}_V(x) = \begin{cases} -1, & \text{if } x \in \Omega, \\ +1, & \text{if } x \in \mathcal{D} \setminus \Omega, \end{cases} \quad (3.6)$$

while the topological derivative of the energy  $\mathcal{T}_E(x)$  is known [75, Ch. 5, pp. 158], whose closed formula is written as (see also [43, 63, 85])

$$\mathcal{T}_E(x) = \mathbb{P}_\gamma \sigma(u(x)) \cdot (\nabla u(x))^s, \quad (3.7)$$

where the polarization tensor  $\mathbb{P}_\gamma$  is given by the following fourth order isotropic tensor

$$\mathbb{P}_\gamma = \frac{1}{2} \frac{1-\gamma}{1+\gamma a_2} \left( (1+a_2)\mathbb{I} + \frac{1}{2}(a_1-a_2) \frac{1-\gamma}{1+\gamma a_1} \mathbf{I} \otimes \mathbf{I} \right), \quad (3.8)$$

with the parameters  $a_1$  and  $a_2$  given by

$$a_1 = \frac{\lambda + \mu}{\mu} \quad \text{and} \quad a_2 = \frac{\lambda + 3\mu}{\lambda + \mu}, \quad (3.9)$$

and the contrast  $\gamma$  defined through (1.5). Let us now present a numerical example concerning the optimal design of a bridge structure. The initial domain shown in Fig. 2 is represented by a rectangular panel  $180 \times 60 \text{ m}^2$ , with Young modulus  $E = 210 \times 10^9 \text{ N/m}^2$  and Poisson ratio  $\nu = 1/3$ , clamped on the region  $a = 9\text{m}$  and submitted to an uniformly distributed traffic loading  $\bar{q} = 250 \times 10^3 \text{ N/m}^2$ . This load is applied on the dark strip of height  $h = 3\text{m}$ , which is placed at an distance  $c = 30\text{m}$  from the top of the design domain. The dark strip will not be optimized. The Lagrange multiplier is fixed as  $\beta = 10 \times 10^6 \text{ N/m}^2$  and the contrast  $\rho_0 = 10^{-4}$ . The topological derivative of the shape functional  $\mathcal{F}_\Omega(u)$  which is obtained in the first iteration

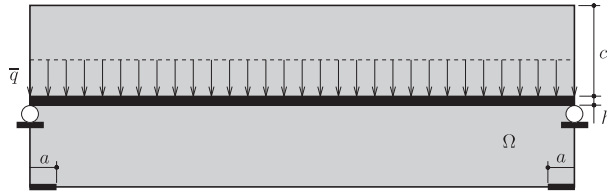


FIGURE 2. Hold-all-domain.

of the shape and topology optimization numerical procedure is shown in Fig. 3, where white to black levels mean smaller (negative) to higher (positive) values. This picture induces a level-set domain representation for the optimal shape, as proposed in [13]. See Algorithm 1. The

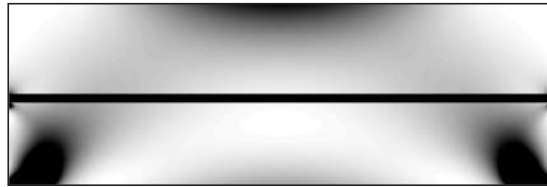


FIGURE 3. Topological derivative in the hold-all domain for the bridge design.

resulting topology design obtained in the form of a well-known tie-arch bridge structure, which is acceptable from practical point of view, is shown in Fig. 4. Usually it is a local minimizer obtained numerically for the compliance minimization with volume constraint. Indeed, there is a lack of sufficient optimality conditions for such shape optimization problems [21]. The convergence curves for the angle  $\theta_n$  and shape functional  $J(\Omega_n)$  is shown in Fig. 5, where the pics come out from the mesh refinement procedure.

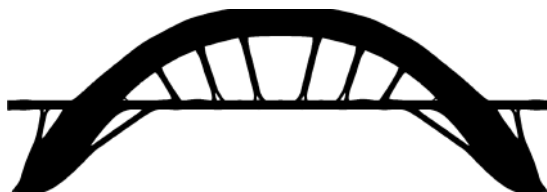


FIGURE 4. Optimal shape for the bridge design [75].

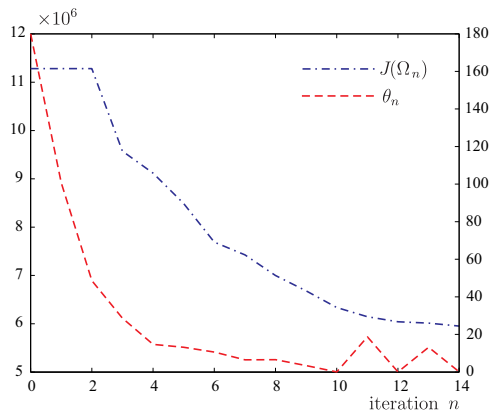


FIGURE 5. Convergence curves for the bridge design: angle  $\theta_n$  (in dashed red line) and shape functional  $J(\Omega_n)$  (in dashed-dot blue line).

Now, let us consider the elasticity boundary value problem into three spatial dimensions, namely  $\mathcal{D} \subset \mathbb{R}^3$ . The topological perturbation we are dealing with consists in the nucleation of a small spherical cavity  $\omega_\varepsilon(x) = B_\varepsilon(x)$ , endowed with homogeneous Neumann boundary condition on  $\partial B_\varepsilon$ . It means that the cavity has a free boundary, so that it represents a void embedded within the elastic body  $\mathcal{D}$ . In this case, the topological derivative of the volume constraint is trivial, while the topological derivative of the energy shape functional is given by

$$\mathcal{T}_E(x) = \mathbb{P}\sigma(u(x)) \cdot (\nabla u(x))^s \quad \forall x \in \mathcal{D}, \quad (3.10)$$

where  $\mathbb{P}$  is the polarization tensor, given in this particular case by the following isotropic fourth order tensor [8]

$$\mathbb{P} = \frac{3}{4} \frac{1-\nu}{7-5\nu} \left( 10\mathbb{I} - \frac{1-5\nu}{1-2\nu} \mathbf{I} \otimes \mathbf{I} \right), \quad (3.11)$$

where  $E$  is the Young's modulus and  $\nu$  the Poisson's ratio. In order to explain briefly the significance of the topological derivative in shape optimization we present one example, with the well known solution obtained by numerical methods. We use a simple procedure consisting in a successive nucleation of cavities where the topological derivative is most negative. In particular, the topology is identified by the strong material distribution and the inclusions of weak material are used to mimic the cavities. In addition, the topological derivative is evaluated at the nodal points of the finite elements mesh. Then, we remove the elements that share the node where the topological derivative assumes its more negative values. This procedure is repeated until the topological derivative becomes positive everywhere. For more elaborated topology design algorithm, the reader may refer to [13]. In particular, let us consider the design of a simply supported cube on the bottom under vertical load applied on the top, as shown in Fig. 6. The details of the obtained results are shown in Fig. 7. This numerical result is due to the former Engineering student Juan Manuel Marmo Lupano and can also be found in [74].

One of the most important requirements in the design of mechanical components is to find the optimal configuration which satisfies a material failure criterion [11, 27, 37, 40, 60, 78]. Following the original ideas presented in [18], let us consider a structural weight minimization problem under stress constraints. We restrict ourselves to the case of an elasticity system into two spatial dimensions, namely  $\mathcal{D} \subset \mathbb{R}^2$ . Therefore, given a hold-all domain  $\mathcal{D}$  and a stress constraints-enforcement sub-domain  $\Omega^* \subset \mathcal{D}$ , the optimization problem we are dealing with consists in finding a subdomain  $\Omega \subset \mathcal{D}$  that solves the following constrained minimization problem:

$$\begin{cases} \text{Minimize } \mathcal{F}_\Omega(u) := |\Omega| + \kappa \mathcal{J}(u) \\ \text{subject to } \sigma_M(u) \leq \bar{\sigma} \quad \text{a.e. in } \Omega^* \subset \Omega \end{cases} \quad (3.12)$$

where  $\kappa > 0$  and the stress constraints are enforced in the relatively compact subdomain  $\Omega^*$  of  $\Omega$ . Finally,  $u$  is solution to the elasticity boundary value problem (3.1) for  $d = 2$ . Therefore,

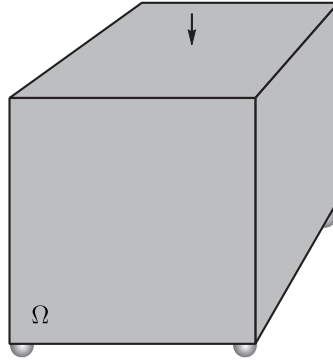


FIGURE 6. Initial guess and boundary conditions for the trestle design problem.

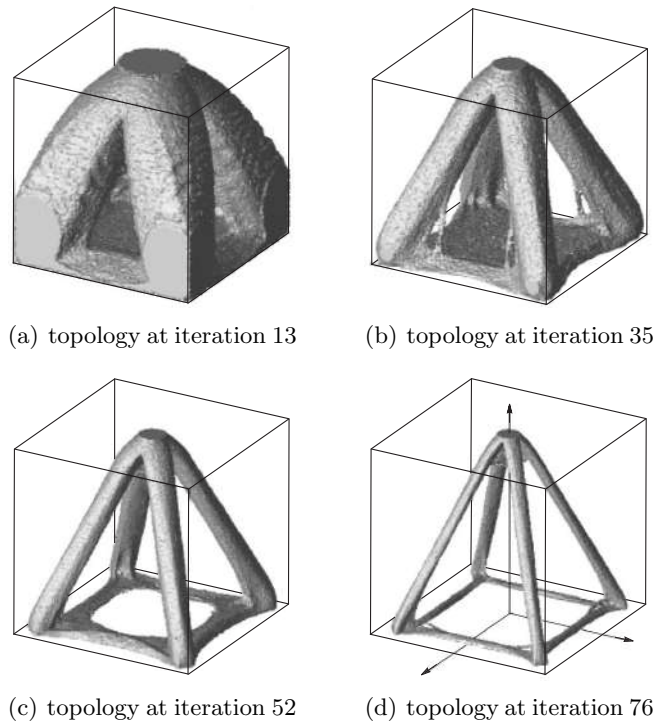


FIGURE 7. History of the trestle topology design problem [74].

the idea is to minimize the volume of the structure under local stress constraints. Since this is an ill-posed problem, the shape functional  $\mathcal{J}(u)$  in (3.12) represents a regularization term given by the structural compliance, namely:

$$\mathcal{J}(u) = \int_{\Gamma_N} \bar{q} \cdot u. \quad (3.13)$$

Some terms in the above expressions still require explanation. The von Mises effective stress  $\sigma_M(u)$  is given by

$$\sigma_M(u) := \sqrt{\frac{1}{2} \mathbb{B} \sigma(u) \cdot \sigma(u)} \quad (3.14)$$

with  $\mathbb{B} = 3\mathbb{I} - \mathbf{I} \otimes \mathbf{I}$ , where  $\mathbb{I}$  and  $\mathbf{I}$  are the fourth and second order identity tensors, respectively. In order to deal with the point-wise stress constraints in (3.12), a class of von Mises stress penalty functional is introduced [18]. It is defined as:

$$\mathcal{G}(u) := \int_{\Omega^*} \Phi_q(\sigma_M^2(u)/\bar{\sigma}^2), \quad (3.15)$$

where  $\Phi_q : \mathbb{R}_+ \rightarrow \mathbb{R}_+$  has the following functional form (for more details the reader may refer to [18, 19]):

$$\Phi_q(t) = [1 + t^q]^{1/q} - 1, \quad (3.16)$$

where the exponent  $q \geq 1$  has to be chosen as large as possible, which is fixed here as  $q = 32$ . For a detailed explanation on how to choose it we refer to the original paper [11]. Therefore, the previous constrained optimization problem (3.12) can be approximated by the following penalized unconstrained optimization problem:

$$\text{Minimize}_{\Omega \subset \mathcal{D}} \mathcal{F}_\Omega^\alpha(u) := \mathcal{F}_\Omega(u) + \alpha \mathcal{G}(u), \quad (3.17)$$

with the scalar  $\alpha > 0$  used to denote a given penalty coefficient. The associated topological derivative  $\mathcal{T}(x)$  of (3.17) can be found in [18], for instance. Let us present a numerical example concerning a standard benchmark, which is solved by using Algorithm 1. It consists in the topology design of a structure with a geometrical singularity. The initial guess is given by a L-shaped beam clamped on the top of the vertical branch, which is submitted to a load applied on the top of the horizontal branch, as shown in Fig. 8. The obtained final topologies are presented in Fig. 9 for the unconstrained and constrained cases. We observe that the reentrant corner is rounded in the constrained case, allowing to keep the stress under control.

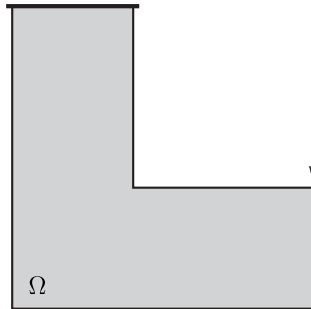


FIGURE 8. Initial guess and boundary conditions for the L-shaped beam design problem.

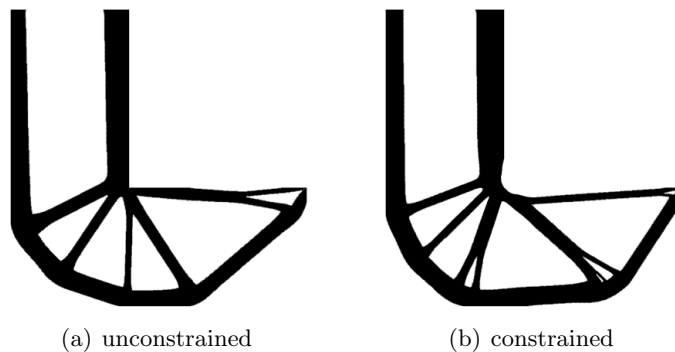


FIGURE 9. Final obtained configurations for the L-shaped beam design problem [18].

Compliant mechanisms are mechanical devices composed by one single part that transforms simple inputs into complex movements by amplifying and changing their direction [3, 29, 31, 61, 66, 68, 83]. A compliant mechanism needs to be stiff enough to support external loads and at the same time must be flexible enough to satisfy the kinematic requirements. Another difficulty that arises is the tendency of forming flexible joints (hinges), in which the stresses exceed the material failure limit. However, there are relatively few papers dealing with compliant mechanisms design under stress constraints [3, 65, 68]. Following the original ideas from [65], let us consider  $\mathcal{D} \subset \mathbb{R}^2$ . The Neumann boundary  $\Gamma_N$  consists of three mutually disjoint parts, that is  $\Gamma_N = \Gamma_{in} \cup \Gamma_{out} \cup \Gamma_0$ , where input, output and zero boundary tractions are prescribed on  $\Gamma_{in}$ ,  $\Gamma_{out}$  and  $\Gamma_0$ , respectively.

Therefore, given a hold-all domain  $\mathcal{D}$  and a stress constraints-enforcement sub-domain  $\Omega^* \subset \mathcal{D}$ , the optimization problem we are dealing with consists in finding a subdomain  $\Omega \subset \mathcal{D}$  that solves the following unconstrained minimization problem:

$$\text{Minimize}_{\Omega \subset \mathcal{D}} \mathcal{F}_{\Omega}^{\alpha}(u) := \beta|\Omega| + \mathcal{J}(u) + \alpha\mathcal{G}(u), \quad (3.18)$$

where  $\beta > 0$ ,  $\alpha > 0$  and  $\Omega^*$  is a relatively compact subdomain of  $\Omega$  where the stress constraints are enforced. In addition, the von Mises penalty functional  $\mathcal{G}(u)$  is given by (3.15). Finally,  $u$  is solution to the elasticity boundary value problem (3.1) for  $d = 2$ . Since the idea is to maximize the output displacement  $u_{out}$  on  $\Gamma_{out}$  for a given input traction on  $\Gamma_{in}$ , the shape functional  $\mathcal{J}(u)$  in (3.18) is defined as [13]:

$$\mathcal{J}(u) = \int_{\Gamma_{in}} q_{in} \cdot u + \kappa \int_{\Gamma_{out}} q_{out} \cdot u, \quad (3.19)$$

where  $q_{in}$  and  $q_{out}$  are given and  $\kappa > 0$  is a penalty coefficient. The associated topological derivative  $\mathcal{T}(x)$  of (3.18) can be found in [65]. In order to fix these ideas, let us present a numerical example, which is solved with help of Algorithm 1. It consists in an inverter mechanism design. The hold-all domain representing the initial guess is given by a rectangle clamped on the left corners, while the loads  $q_{in}$  and  $q_{out}$  are respectively applied on the middle of the left and right edges. See Fig. 10. The amplified deformations of the final obtained configurations are presented in Fig. 11 for the unconstrained and constrained cases. We observe that the obtained mechanisms perform the desired movements. In addition, the constrained case leads to a hinges-free design where the stress is under control.

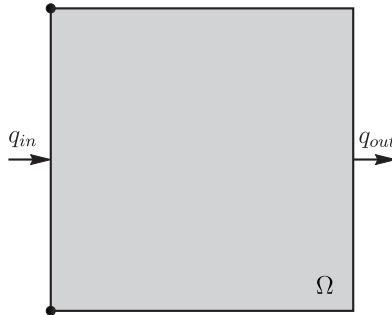


FIGURE 10. Initial guess and boundary conditions for the inverter design problem.

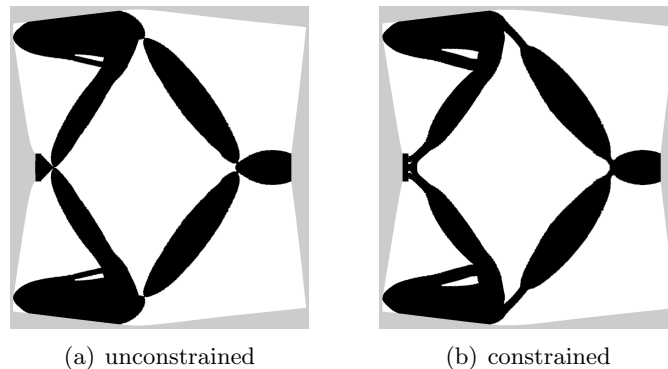


FIGURE 11. Amplified deformation of the final obtained configurations for the inverter design problem [65].

In most cases of practical interest, the parameters of the optimization problem are not deterministic variables. Applied forces intensities, for example, may not be completely known or may

present stochastic variations. Optimization considering uncertainties has been extensively studied in the last decades and several strategies to tackle the problem have been proposed. One interesting branch of research consists in obtaining an optimum design that is least sensitive to variations and uncertainties of the variables, leading to the so-called Robust Optimization. In particular, compliance based robust topology optimization under uncertain loads has been studied in [15, 36, 52, 92], for instance. Here, we follow the ideas presented in [87], where the compliance is evaluated considering a point-wise worst case scenario. Analogously to Sequential Optimization and Reliability Assessment [34], the resulting robust optimization problem can be decoupled into a deterministic topology optimization step and a reliability analysis step. This procedure allows the use of topology optimization algorithms already developed with only small modifications. In particular, since the topological derivative concept has been proved to be robust with respect to uncertainties on the data [56], it has been used to address the deterministic topology optimization problem by using Algorithm 1. The reliability analysis step has been handled as in the Performance Measure Approach [88]. Now, let us consider the design of a tower clamped on the bottom and submitted to a pair of uncertain loads, as shown in Fig. 12. The optimal topologies considering deterministic and uncertain loading are presented in fig. 13.

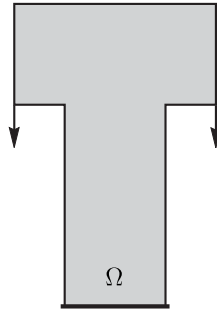


FIGURE 12. Initial guess and boundary conditions for the tower design problem.

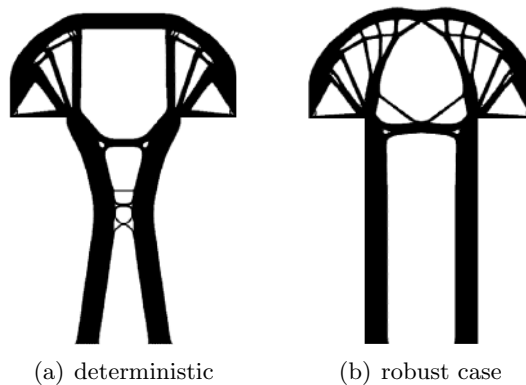


FIGURE 13. Final obtained configurations for the tower design problem [87].

**3.2. Fluid Flow Design.** Let us consider a fluid flow channel design problem. A first work dealing with such a problem was published in [50]. In their work, the topological sensitivity analysis with respect to the insertion of a small hole or obstacle inside a domain has been used to perform the shape optimization considering Stokes equations. The paper [10] extends this work to Navier-Stokes equations by considering an incompressible fluid and a non-slip condition prescribed on the boundary of an arbitrary-shaped obstacle. So far the implemented methods can only create small holes inside the domain. Once these holes have been created, they usually remain unchanged during the topological phase of the optimization algorithm. Thus, in [51] a

bidirectional topological derivative method is introduced, which allows the decision of whether an existing hole must be removed or not for improving the cost function. In addition, in [35] the topological derivative is combined with standard level-set method for the optimal shape design of Stokes flow. More recently, in [80] a new topological derivative formulation for Stokes as well as Navier-Stokes fluid flow channel design has been proposed, which is based on the concept of traditional topology optimization formulations in which solid or fluid material is distributed at each point of the domain to optimize the cost function subject to some constraints. By using this idea, the problem of dealing with the hole boundary conditions during the optimization process is solved because the asymptotic expansion is performed with respect to the nucleation of inclusions – which mimic solid or fluid phases – instead of inserting or removing holes in the fluid domain, which allows for working in a fixed computational domain. For the theoretical development of shape and topology optimization in the context of compressible Navier-Stokes see, for instance, the book [79].

Following the original ideas presented in [80], let us consider a hold-all domain  $\mathcal{D} \subset \mathbb{R}^3$ , which is divided into two subdomains  $\Omega \subset \mathcal{D}$  and  $\mathcal{D} \setminus \Omega$ , which are used to represent the fluid and solid phases, respectively. The topology optimization problem we are dealing with can be written as follows:

$$\text{Minimize}_{\Omega \subset \mathcal{D}} \mathcal{F}_\Omega(u) = \mathcal{J}(u) + \beta|\Omega|, \quad (3.20)$$

where  $\mathcal{J}(u)$  is the energy shape functional, that is

$$\mathcal{J}(u) = \mu \int_{\mathcal{D}} \|\nabla u\|^2 + \int_{\mathcal{D}} \alpha \|u\|^2, \quad (3.21)$$

while  $\beta$  is a fixed multiplier used to impose a volume constraint in  $\Omega$  of the form  $|\Omega| \leq M$ . Some terms of the energy shape functional require explanations. The function  $u$  is solution the Navier-Stokes system combined with Darcy's law, namely: Find  $u$  and  $p$ , such that

$$\begin{cases} -\mu\Delta u + (\nabla u)u + \alpha u + \nabla p = 0 & \text{in } \mathcal{D}, \\ \text{div}(u) = 0 & \text{in } \mathcal{D}, \\ u = u_0 & \text{on } \partial\mathcal{D}, \end{cases} \quad (3.22)$$

where  $u_0 : \int_{\partial\mathcal{D}} u_0 \cdot \nu = 0$ , with  $\nu$  denoting the outward unit normal of the boundary  $\partial\mathcal{D}$ . In addition,  $0 < \mu < \infty$  is the kinematic viscosity and  $\alpha = \alpha(x)$  is the inverse permeability. Therefore, formally  $\alpha \rightarrow 0$  in  $\Omega$  and  $\alpha \rightarrow \infty$  in  $\mathcal{D} \setminus \Omega$ . It means that  $\alpha$  is used to mimic solid or fluid phases, allowing to work on a fixed computation domain. The topological perturbation we are dealing with is defined by  $\alpha_\varepsilon = \gamma_\varepsilon \alpha$ , where  $\gamma_\varepsilon$  is defined in (1.4). In this case, the topological derivative of the energy shape functional is given by

$$\mathcal{T}_E(x) = -(1 - \gamma)\alpha(x)u(x) \cdot (u(x) - v(x)) \quad \forall x \in \mathcal{D}, \quad (3.23)$$

while the topological derivative of the volume constraint is trivial. Finally, the auxiliary vector function  $v$  is solution to the following adjoint problem: Find  $v$  and  $q$ , such that

$$\begin{cases} -\mu\Delta v + (\nabla u)^\top v - (\nabla v)u + \alpha v + \nabla q = 2(\alpha u - \mu\Delta u) & \text{in } \mathcal{D}, \\ \text{div}(v) = 0 & \text{in } \mathcal{D}, \\ v = 0 & \text{on } \partial\mathcal{D}. \end{cases} \quad (3.24)$$

Based on the above ideas, let us present an example of fluid flow design into three spatial dimensions. It consists in a three-way channel problem, with two inlets, one normal to the X axis and the other one normal to the Y axis, and one outlet, normal to the Z axis. Unitary parabolic profiles for the velocity are imposed in the inlets, while in the outlet there is zero pressure. See sketch in Fig. 14. The obtained result is shown in Fig. 15, where Algorithm 1 has been applied.

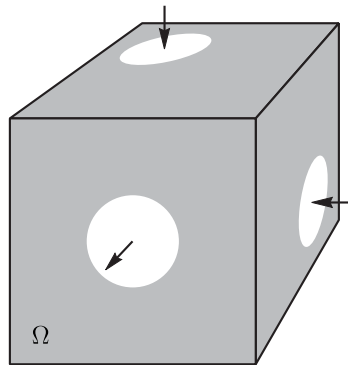


FIGURE 14. Design domain for three way channel design problem.

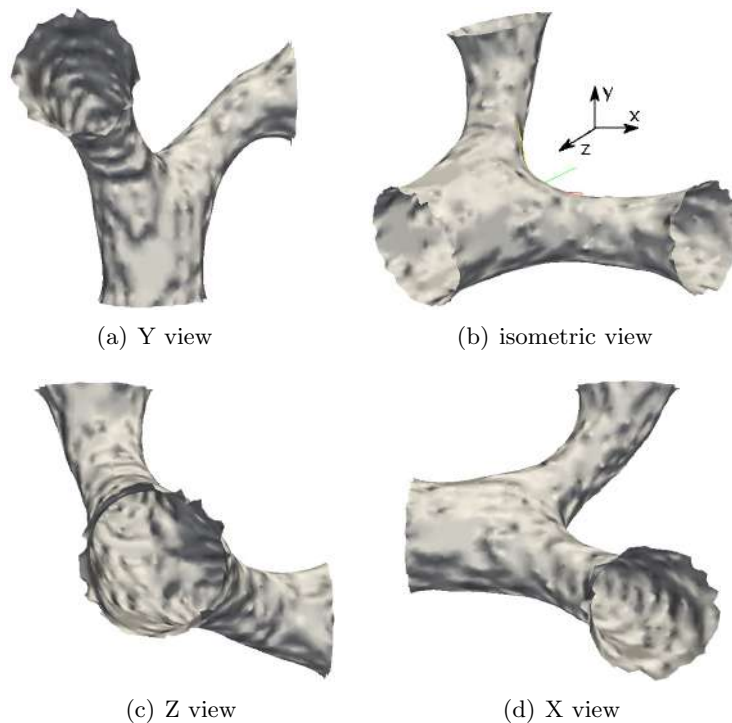


FIGURE 15. Final topology (fluid domain) for the three way channel design problem [80].

**3.3. Multiscale Material Design.** Following the original ideas presented in [46] and further developed in [17], a multiscale material design methodology is presented. It relies on an exact formula for the sensitivity of the macroscopic elasticity tensor to topological microstructural changes. See also [45, 47, 67, 76]. In particular, the associated sensitivity is given by a symmetric fourth order tensor field over the Representative Volume Element (RVE) that measures how the macroscopic elasticity constants estimated within the multiscale framework changes when a small circular hole is introduced at the microscale level. It is derived by making use of the notion of topological derivatives within the variational formulation of well-established multiscale constitutive theory fully developed in the book by Sanchez-Palencia 1980 [82] (see also [44, 69, 70]), where the macroscopic strain and stress tensors are volume averages of their microscopic counterparts over the RVE. The final format of the proposed analytical formula is strikingly simple, so that it is used to devise a topology design algorithm for the synthesis and optimal design of microstructures to meet a specified macroscopic behavior [17]. In particular,

we are interested in the synthesis of microstructures of standard material to produce auxetic macrostructures.

Let us consider a macroscopic domain  $\Omega \subset \mathbb{R}^2$ . Associated with any point  $x \in \Omega$  there is a local RVE whose domain is denoted by  $\Omega_\mu$ , with boundary  $\partial\Omega_\mu$ . The homogenized elasticity tensor  $\mathbb{C}$  is defined as

$$(\mathbb{C})_{ijkl} = \frac{1}{V_\mu} \int_{\Omega_\mu} (\sigma_\mu(u_\mu^{kl}))_{ij}, \quad (3.25)$$

where  $V_\mu$  denotes the total volume of the RVE and  $u_\mu^{kl}$  is given by

$$u_\mu^{kl}(y) := u + (e_k \otimes e_l)y + \tilde{u}_\mu^{kl}(y). \quad (3.26)$$

The constant (rigid) RVE displacement coinciding with the macroscopic displacement field  $u$  at the point  $x \in \Omega$ . The microscopic displacement fluctuation field  $\tilde{u}_\mu^{kl}$  is solution to the following canonical set of variational problems [82]: Find  $\tilde{u}_\mu^{kl} \in \mathcal{V}_\mu$ , such that

$$\int_{\Omega_\mu} \sigma_\mu(\tilde{u}_\mu^{kl}) \cdot \varepsilon_\mu(\eta) + \int_{\Omega_\mu} \mathbb{C}_\mu(e_k \otimes_s e_l) \cdot \varepsilon_\mu(\eta) = 0 \quad \forall \eta \in \mathcal{V}_\mu, \quad (3.27)$$

with  $\sigma_\mu(\tilde{u}_\mu^{kl}) = \mathbb{C}_\mu \varepsilon_\mu(\tilde{u}_\mu^{kl})$ , where  $\varepsilon_\mu(\eta)$  is the symmetric part of the gradient of  $\eta$ . The microscopic constitutive tensor  $\mathbb{C}_\mu$  written in terms of the Lamé's coefficients  $\mu$  and  $\lambda$  is given by  $\mathbb{C}_\mu = 2\mu\mathbb{I} + \lambda\mathbb{I} \otimes \mathbb{I}$ , with  $\mathbb{I}$  and  $\mathbb{II}$  used to denote the second and fourth order identity tensors, respectively. The complete characterization of the multiscale constitutive model is obtained by defining the subspace  $\mathcal{V}_\mu \subset \mathcal{U}_\mu$  of kinematically admissible displacement fluctuations. In general, different choices produce different macroscopic responses for the same RVE. In this work we restrict ourselves to media with periodic microstructure. In this case, the geometry of the RVE cannot be arbitrary and must represent a cell whose periodic repetition generates the macroscopic continuum. In addition, the displacement fluctuations must satisfy periodicity on the boundary of the RVE. Accordingly, we have

$$\mathcal{V}_\mu := \{ \varphi \in \mathcal{U}_\mu : \varphi(y^+) = \varphi(y^-) \quad \forall (y^+, y^-) \in \mathfrak{P} \}, \quad (3.28)$$

where  $\mathfrak{P}$  is the set of pairs of points, defined by a one-to-one periodicity correspondence, lying on opposing sides of the RVE boundary. Finally, the minimally constrained space of kinematically admissible displacements  $\mathcal{U}_\mu$  is defined as

$$\mathcal{U}_\mu := \left\{ \varphi \in H^1(\Omega_\mu) : \int_{\Omega_\mu} \varphi = 0, \int_{\partial\Omega_\mu} \varphi \otimes_s n = 0 \right\}. \quad (3.29)$$

where  $n$  is the outward unit normal to the boundary  $\partial\Omega_\mu$  and  $\otimes_s$  denotes the symmetric tensor product between vectors. A closed formula for the sensitivity of the homogenized elasticity tensor (3.25) to the nucleation of a circular hole within the RVE has been derived in [46]. It is given the following fourth order tensor field over  $\Omega_\mu$

$$\mathbb{D}_\mu(y) = -\frac{1}{V_\mu} \mathbb{P}_\mu \sigma_\mu(u_\mu^{ij}(y)) \cdot \sigma_\mu(u_\mu^{kl}(y)) e_i \otimes e_j \otimes e_k \otimes e_l \quad \forall y \in \Omega_\mu, \quad (3.30)$$

with the polarization tensor  $\mathbb{P}_\mu$  given by

$$\mathbb{P}_\mu = \frac{2\mu + \lambda}{3\mu + \lambda} \left( \mathbb{I} + \frac{\mu - \lambda}{4(\mu + \lambda)} \mathbb{I} \otimes \mathbb{I} \right), \quad (3.31)$$

where the fields  $u_\mu^{ij}$  come out from the solutions to (3.27) for the unperturbed RVE domain  $\Omega_\mu$  together with the additive decomposition (3.26). Expression (3.30) allows the exact topological derivative of any differentiable function of  $\mathbb{C}$  be calculated through the direct application of the conventional rules of differential calculus. That is, any such a function  $\Psi(\mathbb{C})$  has exact topological derivative of the form

$$\mathcal{T}_\mu = \langle D\Psi(\mathbb{C}), \mathbb{D}_\mu \rangle, \quad (3.32)$$

with the brackets  $\langle \cdot, \cdot \rangle$  denoting the appropriate product between the derivative of  $\Psi$  with respect to  $\mathbb{C}$  and the topological derivative  $\mathbb{D}_\mu$  of  $\mathbb{C}$ . Note, for example, that properties of interest

such as the homogenized Young's, shear and bulk moduli as well as the Poisson ratio are all regular functions of  $\mathbb{C}$ . This fact points strongly to the suitability of the use of (3.32) in a topology algorithm for the synthesis and optimization of elastic micro-structures based on the minimization/maximization of cost functions defined in terms of homogenized properties. In order to fix these ideas, let us consider the pair  $\varphi_1, \varphi_2 \in \mathbb{R}^2 \times \mathbb{R}^2$  of second order tensors. We also introduce the quantity

$$\Psi(\mathbb{C}) := \frac{\mathbb{C}^{-1}\varphi_1 \cdot \varphi_2}{\mathbb{C}^{-1}\varphi_1 \cdot \varphi_1} + \frac{\mathbb{C}^{-1}\varphi_2 \cdot \varphi_1}{\mathbb{C}^{-1}\varphi_2 \cdot \varphi_2}. \quad (3.33)$$

Then the following result, which can be used in numerical methods of synthesis and/or topology design of microstructures [17], holds true:

$$\mathcal{T}_\mu = - \frac{(\mathbb{C}^{-1}\mathbb{D}_\mu\mathbb{C}^{-1})\varphi_1 \cdot [(\mathbb{C}^{-1}\varphi_1 \cdot \varphi_1)\varphi_2 - (\mathbb{C}^{-1}\varphi_1 \cdot \varphi_2)\varphi_1]}{(\mathbb{C}^{-1}\varphi_1 \cdot \varphi_1)^2} - \frac{(\mathbb{C}^{-1}\mathbb{D}_\mu\mathbb{C}^{-1})\varphi_2 \cdot [(\mathbb{C}^{-1}\varphi_2 \cdot \varphi_2)\varphi_1 - (\mathbb{C}^{-1}\varphi_2 \cdot \varphi_1)\varphi_2]}{(\mathbb{C}^{-1}\varphi_2 \cdot \varphi_2)^2}. \quad (3.34)$$

Finally, let us consider one RVE given by a unit square  $\Omega_\mu = (0, 1) \times (0, 1)$ . The initial guess is given by a porous microcell as shown in Fig. 16. By setting  $\varphi_1 = e_1 \otimes e_1$  and  $\varphi_2 = -e_2 \otimes e_2$  in (3.33), the resulting function  $\Psi(\mathbb{C})$  yields

$$\Psi(\mathbb{C}) := - \frac{(\mathbb{C}^{-1})_{1122}}{(\mathbb{C}^{-1})_{1111}} - \frac{(\mathbb{C}^{-1})_{1122}}{(\mathbb{C}^{-1})_{2222}}. \quad (3.35)$$

The obtained optimized auxetic microstructure is presented in Fig. 17(a), while the resulting periodic auxetic structure is shown in Fig. 17(b). These results have been obtained with help of Algorithm 1.

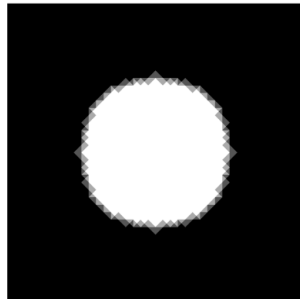


FIGURE 16. Initial guess for the auxetic microstructure material design.

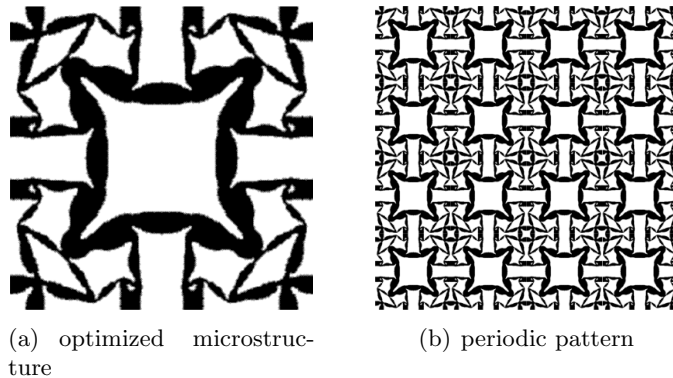


FIGURE 17. Obtained result for the auxetic microstructure material design [17].

**3.4. Additional Applications.** In this section we discuss some additional applications found in the current literature. We do not give details, but the problems are presented in words and precise references are given for the reader convenience.

**3.4.1. Antenna Design in Hyperthermia Therapy.** Hyperthermia is a non-invasive therapy, commonly used in treatment of cancer, consisting in artificially heating body tissue through electromagnetic waves by focusing the heat in cancerous cells. However, one of the challenges in the hyperthermia treatment is to selectively heat the cancerous tissue, elevating its temperature above  $42^{\circ}\text{C}$ , while keeping the temperatures of the healthy tissue close to the normal temperature of the human body. In this scenario, the applied heat may damage or even kill first the cancerous cells. Even if the cancerous cells do not die immediately, they may become more vulnerable to radiotherapy or chemotherapy, enabling such – in general aggressive – therapies to be given in smaller doses. The regional electromagnetic hyperthermia problem is modeled by a semi-coupled system of partial differential equations. The heat equation in biologic tissues, or *bioheat equation*, is coupled with the *Helmholtz equation*. Electromagnetic waves are generated by spatially distributed antenna. This antenna produces a source in the Helmholtz equation, whose solution appears as a heat source in the bioheat equation. Therefore, the basic idea consists in finding a distribution of heat source generated by electromagnetic antenna, which is able to focus the heat into the tumor and keep the temperature under control in the healthy tissue. In other words, the support of the antenna has to be designed, leading to a topology optimization problem. In the work [5], the problem has been successfully solved with help of the topological derivative concept. In particular, the authors presented some numerical results showing possible application of the proposed methodology to the cancer treatment by hyperthermia.

**3.4.2. Inverse Scattering Problem.** The topological derivative associated with the Helmholtz problem [81] has been successfully applied for imaging small acoustic anomalies [41]. The basic idea consists in minimizing a shape functional measuring the misfit between the boundary measurements and the solution obtained from the model by using the topological derivative concept. In particular, the topological derivative field obtained from the background solution gives qualitative information on the shape and topology of the hidden anomalies. See also [16, 32, 42, 53, 57], for instance. See also an experimental validation of the topological derivative method in the context of elastic-wave imaging [86]. The stability and resolution analysis for a topological derivative based imaging functional has been presented in [7], showing why it works so well in the context of inverse scattering. See also an application of the topological derivative concept in the context of AFM-based indentation stiffness tomography [22].

**3.4.3. Crack Nucleation Modeling.** A simple analytical expression for crack nucleation sensitivity analysis has been derived in [90]. See also [9]. It relies on the concept of topological derivative applied within a two-dimensional linear elastic fracture mechanics theory. In particular, the topological asymptotic expansion of the total potential energy together with a Griffith-type energy of an elastic cracked body has been calculated. As main result, a crack nucleation criterion based on the topological derivative and a criterion for determining the direction of crack growth based on the associated topological gradient have been introduced.

**3.4.4. Damage Evolution Modeling.** The topological derivative associated with the Francfort-Marigo model of damage evolution in brittle materials has been used to nucleate small damaged zones. After nucleating new damages, a level-set method has been used to propagate them according to the associated shape derivative of the Francfort-Marigo functional. For more details, see [4]. However, the whole nucleation and propagation damaging process, including kinking and bifurcation, can also be modeled by using solely the topological derivative concept, leading to a simple and unified approach for such a phenomenon [91].

**3.4.5. Imaging Processing.** As a consequence of the technological advance a variety of instruments and tools have been introduced in medicine. For instance, we can refer to medical imaging devices. More specifically, techniques like Computed Tomography, Magnetic Resonance Imaging, Single Photon Emission Tomography, Positron Emission Tomography and Ultrasound

among others, have provided useful information (anatomical and functional) to specialists, no matter which is the area of interest (practical medicine, research, etc.). Therefore, the demand for tools to manipulate medical images has grown considerably since the appearance of these technologies. Also different issues have appeared in this field, and to recall some of them we can mention volume data visualization, image restoration, image segmentation, image registration, pattern recognition and inpainting. The topological derivative concept has been successfully applied for solving such a class of imaging processing problems, including the so-called minimal partition problem [20]. See, for instance, [23, 24, 54, 55, 59]. See also the recent publications [33, 71].

#### 4. PERSPECTIVES AND OPEN PROBLEMS

In this second part of review on the topological derivatives, the topology optimization algorithm with the first order topological derivative and the level-set domain representation method is presented. The large set of applications in the context of topology optimization is provided. General algorithm 1 has been proposed in [13] to achieve a local optimality condition for the minimization problem under considerations. The local optimality conditions for topology optimization problems are given in terms of the topological derivatives and appropriate level-set functions. This means that the topological derivative is in fact used within the numerical procedure as a steepest-descent direction. Therefore, we propose the class of optimization processes similar to methods based on the gradient of the cost functional. The topological derivative represents the variation of the shape functional with respect to the nucleation of small singular domain perturbations, so that the resulting topology design algorithm converges in few iterations by using a small number of user defined algorithmic parameters. Furthermore, the topological derivative follows in fact the basic rules of Differential Calculus, so that it can be applied in the context of multi-objective topology optimization algorithms by using e.g., the known formulas already available in the literature. Finally, in contrast to traditional topology optimization methods, the topological derivative formulation does not require any material model concept based on intermediary densities, so that no interpolation schemes are used within the numerical procedures. This feature is crucial in the topology design problem, since the difficulties arising from material model procedures are here naturally avoided. Therefore, the topological derivative method can be seen, when applicable, as a simple alternative method for numerical solution of a wide class of topology optimization problems. For future developments of shape-topological first order method we highlight:

- (1) According to Section 3, there are numerical evidences showing that Algorithm 1 converges in most cases. However, from the theoretical point of view, only partial results can be found in the literature. See for instance [12], where the convergence analysis of Algorithm 1 has been studied in the particular case of optimal control problem with respect to characteristic functions of small sets. Therefore, the most important theoretical problem to be solved concerns the convergence analysis of Algorithm 1.
- (2) The stability and resolution analysis for a topological derivative based imaging functional has been presented in the context of Helmholtz equation [7]. However, such an analysis is missing for other classes of inverse problems, including gravimetry and EIT, for instance.
- (3) Design of metamaterials in a multiscale framework has been considered in [46], where the topological derivative of the homogenized elasticity tensor has been obtained. The extension to the strain gradient homogenized constitutive tensor is a difficult and interesting research topic.
- (4) Topological derivative-based topology design in multiphysics taking into account multi-objective shape functionals is an important and difficult subject of research, which also deserves investigation. Design of antenna and wave guides in nanophotonics is an example of application. It can be deal with the domain decomposition technique presented in the first part of this series of review papers.
- (5) The Griffith-Francfort-Marigo damage model adopted in [4] does not distinguish the difference between traction and compression stress states in the damage evolution process.

Hence, it is not suited to describe the crack closure phenomenon. Therefore, the development of the topological derivative for functionals which specifically would consider distinct criteria in traction and in compression deserves investigation. However, it is well-known that such a modeling leads to a class of non-linear elasticity systems, so that the difficulty arising from these extensions have to be considered.

- (6) The extension to non-linear problems in general can be considered as the main challenge associated with the theoretical development of the topological derivative method. The difficulty arises when the non-linearity comes out from the main part of the operator, which at the same time suffers a topological perturbation. It is the case of nucleation of holes in plasticity and finite deformations in solid mechanics, for instance. See recent publication [14] dealing with topological derivatives for a class of quasilinear elliptic equations.

#### AACKNOWLEDGEMENTS

This research was partly supported by CNPq (Brazilian Research Council), CAPES (Brazilian Higher Education Staff Training Agency) and FAPERJ (Research Foundation of the State of Rio de Janeiro). These supports are gratefully acknowledged. We would also like to thank Samuel Amstutz, Sebastián Giusti, Nicolas Van Goethem, Eduardo Neto, Luís Fernando Sá, Emílio Silva, André Torii, and the former students Alan Amad, Cinthia Lopes, Renatha Santos and Marcel Xavier.

#### REFERENCES

- [1] G. Allaire. *Conception optimale de structures*, volume 58 of *Mathématiques et applications*. Springer-Verlag, Berlin, 2007.
- [2] G. Allaire, F. de Gournay, F. Jouve, and A. M. Toader. Structural optimization using topological and shape sensitivity via a level set method. *Control and Cybernetics*, 34(1):59–80, 2005.
- [3] G. Allaire, F. Jouve, and H. Maillot. Minimum stress optimal design with the level-set method. *Engineering Analysis with Boundary Elements*, 32(11):909–918, 2008.
- [4] G. Allaire, F. Jouve, and N. Van Goethem. Damage and fracture evolution in brittle materials by shape optimization methods. *Journal of Computational Physics*, 230(12):5010–5044, 2011.
- [5] A. A. S. Amad, A. F. D. Loula, and A. A. Novotny. A new method for topology design of electromagnetic antennas in hyperthermia therapy. *Applied Mathematical Modelling*, 42:209–222, 2017.
- [6] R. C. R. Amigo, S.M. Giusti, A. A. Novotny, E. C. N. Silva, and J. Sokolowski. Optimum design of flexensional piezoelectric actuators into two spatial dimensions. *SIAM Journal on Control Optimization*, 52(2):760–789, 2016.
- [7] H. Ammari, J. Garnier, V. Jugnon, and H. Kang. Stability and resolution analysis for a topological derivative based imaging functional. *SIAM Journal on Control and Optimization*, 50(1):48–76, 2012.
- [8] H. Ammari and H. Kang. *Polarization and moment tensors with applications to inverse problems and effective medium theory*. Applied Mathematical Sciences vol. 162. Springer-Verlag, New York, 2007.
- [9] H. Ammari, H. Kang, H. Lee, and J. Lim. Boundary perturbations due to the presence of small linear cracks in an elastic body. *Journal of Elasticity*, 113:75–91, 2013.
- [10] S. Amstutz. The topological asymptotic for the Navier-Stokes equations. *ESAIM: Control, Optimisation and Calculus of Variations*, 11(3):401–425, 2005.
- [11] S. Amstutz. A penalty method for topology optimization subject to a pointwise state constraint. *ESAIM: Control, Optimisation and Calculus of Variations*, 16(3):523–544, 2010.
- [12] S. Amstutz. Analysis of a level set method for topology optimization. *Optimization Methods and Software*, 26(4-5):555–573, 2011.
- [13] S. Amstutz and H. Andrä. A new algorithm for topology optimization using a level-set method. *Journal of Computational Physics*, 216(2):573–588, 2006.
- [14] S. Amstutz and A. Bonnafé. Topological derivatives for a class of quasilinear elliptic equations. *Journal de Mathématiques Pures et Appliquées*, 107:367–408, 2017.
- [15] S. Amstutz and M. A. Ciligot-Travain. A notion of compliance robustness in topology optimization. *ESAIM: Control, Optimisation and Calculus of Variations*, 22(1):64–87, 2016.
- [16] S. Amstutz and N. Dominguez. Topological sensitivity analysis in the context of ultrasonic non-destructive testing. *Engineering Analysis with Boundary Elements*, 32(11):936–947, 2008.
- [17] S. Amstutz, S. M. Giusti, A. A. Novotny, and E. A. de Souza Neto. Topological derivative for multi-scale linear elasticity models applied to the synthesis of microstructures. *International Journal for Numerical Methods in Engineering*, 84:733–756, 2010.

- [18] S. Amstutz and A. A. Novotny. Topological optimization of structures subject to von Mises stress constraints. *Structural and Multidisciplinary Optimization*, 41(3):407–420, 2010.
- [19] S. Amstutz, A. A. Novotny, and E. A. de Souza Neto. Topological derivative-based topology optimization of structures subject to Drucker-Prager stress constraints. *Computer Methods in Applied Mechanics and Engineering*, 233–236:123–136, 2012.
- [20] S. Amstutz, A. A. Novotny, and N. Van Goethem. Minimal partitions and image classification using a gradient-free perimeter approximation. *Inverse Problems and Imaging*, 8(2):361–387, 2014.
- [21] S. Amstutz and N. Van Goethem. Topology optimization methods with gradient-free perimeter approximation. *Inverse Problems and Imaging*, 14(3):401–430, 2012.
- [22] I. I. Argatov. AFM-based indentation stiffness tomography - an asymptotic model. *Journal of the Mechanics and Physics of Solids*, 70:190–199, 2014.
- [23] D. Auroux, M. Masmoudi, and L. Belaid. Image restoration and classification by topological asymptotic expansion. In *Variational formulations in mechanics: theory and applications*, Barcelona, Spain, 2007.
- [24] L. J. Belaid, M. Jaoua, M. Masmoudi, and L. Siala. Application of the topological gradient to image restoration and edge detection. *Engineering Analysis with Boundary Elements*, 32:891–899, 2008.
- [25] M. P. Bendsøe and O. Sigmund. *Topology optimization. Theory, methods and applications*. Springer-Verlag, Berlin, 2003.
- [26] D. Bojczuk and Z. Mróz. Topological sensitivity derivative and finite topology modifications: application to optimization of plates in bending. *Structural and Multidisciplinary Optimization*, 39:1–15, 2009.
- [27] M. Bruggi and P. Duysinx. Topology optimization for minimum weight with compliance and stress constraints. *Structural and Multidisciplinary Optimization*, 46(3):369–384, 2012.
- [28] M. Burger, B. Hackl, and W. Ring. Incorporating topological derivatives into level set methods. *Journal of Computational Physics*, 194(1):344–362, 2004.
- [29] R. H. Burns and F. R. E. Crossley. Kinetostatic synthesis of flexible link mechanisms. *ASME-Paper*, 68(36), 1964.
- [30] D. E. Campêão, S. M. Giusti, and A. A. Novotny. Topology design of plates considering different volume control methods. *Engineering Computations*, 31(5):826–842, 2014.
- [31] E. L. Cardoso and J. S. O. Fonseca. Strain energy maximization approach to the design of fully compliant mechanisms using topology optimization. *Latin American Journal of Solids and Structures*, 1:263–275, 2004.
- [32] A. Carpio and M-L. Rapún. Solving inhomogeneous inverse problems by topological derivative methods. *Inverse Problems*, 24(4):045014, 2008.
- [33] A. Drogoul and G. Aubert. The topological gradient method for semi-linear problems and application to edge detection and noise removal. *Inverse Problems and Imaging*, 10(1):51–86, 2016.
- [34] X. Du and W. Chen. Sequential optimization and reliability assessment method for efficient probabilistic design. *ASME Journal of Mechanical Design*, 126(2):225–233, 2004.
- [35] X. Duan and F. Li. Material distribution resembled level set method for optimal shape design of stokes flow. *Applied Mathematics and Computation*, 266:21–30, 2015.
- [36] P. Dunning and H. Kim. Robust topology optimization: Minimization of expected and variance of compliance. *American Institute of Aeronautics and Astronautics Journal*, 51(11):2656–2664, 2013.
- [37] H. Emmendoerfer Jr. and E. A. Fancello. A level set approach for topology optimization with local stress constraints. *International Journal for Numerical Methods in Engineering*, 99:129–156, 2014.
- [38] H. A. Eschenauer, V. V. Koblelev, and A. Schumacher. Bubble method for topology and shape optimization of structures. *Structural Optimization*, 8(1):42–51, 1994.
- [39] H. A. Eschenauer and N. Olhoff. Topology optimization of continuum structures: a review. *Applied Mechanics Reviews*, 54(4):331–390, 2001.
- [40] E. A. Fancello. Topology optimization of minimum mass design considering local failure constraints and contact boundary conditions. *Structural and Multidisciplinary Optimization*, 32:229–240, 2006.
- [41] G. R. Feijóo. A new method in inverse scattering based on the topological derivative. *Inverse Problems*, 20(6):1819–1840, 2004.
- [42] J. F. Funes, J. M. Perales, M. L. Rapún, and J. M. Manuel Vega. Defect detection from multi-frequency limited data via topological sensitivity. *Journal of Mathematical Imaging and Vision*, 55:19–35, 2016.
- [43] S. Garreau, Ph. Guillaume, and M. Masmoudi. The topological asymptotic for PDE systems: the elasticity case. *SIAM Journal on Control and Optimization*, 39(6):1756–1778, 2001.
- [44] P. Germain, Q. S. Nguyen, and P. Suquet. Continuum thermodynamics. *Journal of Applied Mechanics, Transactions of the ASME*, 50(4):1010–1020, 1983.
- [45] S. M. Giusti, A. A. Novotny, and E. A. de Souza Neto. Sensitivity of the macroscopic response of elastic microstructures to the insertion of inclusions. *Proceeding of the Royal Society A: Mathematical, Physical and Engineering Sciences*, 466:1703–1723, 2010.
- [46] S. M. Giusti, A. A. Novotny, E. A. de Souza Neto, and R. A. Feijóo. Sensitivity of the macroscopic elasticity tensor to topological microstructural changes. *Journal of the Mechanics and Physics of Solids*, 57(3):555–570, 2009.

- [47] S. M. Giusti, A. A. Novotny, E. A. de Souza Neto, and R. A. Feijóo. Sensitivity of the macroscopic thermal conductivity tensor to topological microstructural changes. *Computer Methods in Applied Mechanics and Engineering*, 198(5–8):727–739, 2009.
- [48] S. M. Giusti, A. A. Novotny, and J. Sokółowski. Topological derivative for steady-state orthotropic heat diffusion problem. *Structural and Multidisciplinary Optimization*, 40(1):53–64, 2010.
- [49] S.M. Giusti, Z. Mróz, J. Sokółowski, and A.A. Novotny. Topology design of thermomechanical actuators. *Structural and Multidisciplinary Optimization*, 55:1575–1587, 2017.
- [50] P. Guillaume and K. Sid Idris. Topological sensitivity and shape optimization for the Stokes equations. *SIAM Journal on Control and Optimization*, 43(1):1–31, 2004.
- [51] PH. Guillaume and M. Hassine. Removing holes in topological shape optimization. *ESAIM: Control, Optimisation and Calculus of Variations*, 14(1):160–191, 2008.
- [52] X. Guo, W. Bai, W. Zhang, and X. Gao. Confidence structural robust design and optimization under stiffness and load uncertainties. *Computer Methods in Applied Mechanics and Engineering*, 198(41–44):3378–3399, 2009.
- [53] B. B. Guzina and M. Bonnet. Small-inclusion asymptotic of misfit functionals for inverse problems in acoustics. *Inverse Problems*, 22(5):1761–1785, 2006.
- [54] M. Hintermüller. Fast level set based algorithms using shape and topological sensitivity. *Control and Cybernetics*, 34(1):305–324, 2005.
- [55] M. Hintermüller and A. Laurain. Multiphase image segmentation and modulation recovery based on shape and topological sensitivity. *Journal of Mathematical Imaging and Vision*, 35:1–22, 2009.
- [56] I. Hlaváček, A. A. Novotny, J. Sokółowski, and A. Žochowski. On topological derivatives for elastic solids with uncertain input data. *Journal of Optimization Theory and Applications*, 141(3):569–595, 2009.
- [57] M. Jleli, B. Samet, and G. Vial. Topological sensitivity analysis for the modified Helmholtz equation under an impedance condition on the boundary of a hole. *Journal de Mathématiques Pures et Appliquées*, 103:557–574, 2015.
- [58] V. Kobelev. Bubble-and-grain method and criteria for optimal positioning inhomogeneities in topological optimization. *Structural and Multidisciplinary Optimization*, 40(1-6):117–135, 2010.
- [59] I. Larrabide, R. A. Feijóo, A. A. Novotny, and E. Taroco. Topological derivative: a tool for image processing. *Computers & Structures*, 86(13–14):1386–1403, 2008.
- [60] C. Le, J. Norato, and T. Bruns. Stress-based topology optimization for continua. *Structural Multidisciplinary Optimization*, 41:605–620, 2010.
- [61] E. Lee and H. C. Gea. A strain based topology optimization method for compliant mechanism design. *Structure and Multidisciplinary Optimization*, 49:199–207, 2014.
- [62] G. Leugering and J. Sokółowski. Topological derivatives for elliptic problems on graphs. *Control and Cybernetics*, 37:971–998, 2008.
- [63] T. Lewinski and J. Sokółowski. Energy change due to the appearance of cavities in elastic solids. *International Journal of Solids and Structures*, 40(7):1765–1803, 2003.
- [64] C. G. Lopes, R. B. dos Santos, and A. A. Novotny. Topological derivative-based topology optimization of structures subject to multiple load-cases. *Latin American Journal of Solids and Structures*, 12:834–860, 2015.
- [65] C. G. Lopes and A. A. Novotny. Topology design of compliant mechanisms with stress constraints based on the topological derivative concept. *Structural and Multidisciplinary Optimization*, 54(4):737–746, 2016.
- [66] J. Luo, Z. Luo, S. Chen, L. Tong, and M. Yu Wang. A new level set method for systematic design of hinge-free compliant mechanisms. *Computer Methods in Applied Mechanics and Engineering*, 198:318–331, 2008.
- [67] C. G. Méndez, J. M. Podestá, O. Lloberas-Valls, S. Toro, A. E. Huespe, and J. Oliver. Computational material design for acoustic cloaking. *International Journal for Numerical Methods in Engineering*, 2017, to appear.
- [68] L. R. Meneghelli and E. L. Cardoso. Design of compliant mechanisms with stress constraints using topology optimization. *Optimization of Structures and Components, Advanced Structured Materials*, 43, 2013.
- [69] J. C. Michel, H. Moulinec, and P. Suquet. Effective properties of composite materials with periodic microstructure: a computational approach. *Computer Methods in Applied Mechanics and Engineering*, 172(1–4):109–143, 1999.
- [70] C. Miehe, J. Schotte, and J. Schröder. Computational micro-macro transitions and overall moduli in the analysis of polycrystals at large strains. *Computational Materials Science*, 16(1–4):372–382, 1999.
- [71] M. Muszkiet. A variational approach to edge detection. *Inverse Problems and Imaging*, 10(2):499–517, 2016.
- [72] A. A. Novotny, R. A. Feijóo, C. Padra, and E. Taroco. Topological sensitivity analysis. *Computer Methods in Applied Mechanics and Engineering*, 192(7–8):803–829, 2003.
- [73] A. A. Novotny, R. A. Feijóo, C. Padra, and E. Taroco. Topological derivative for linear elastic plate bending problems. *Control and Cybernetics*, 34(1):339–361, 2005.
- [74] A. A. Novotny, R. A. Feijóo, E. Taroco, and C. Padra. Topological sensitivity analysis for three-dimensional linear elasticity problem. *Computer Methods in Applied Mechanics and Engineering*, 196(41–44):4354–4364, 2007.
- [75] A. A. Novotny and J. Sokółowski. *Topological derivatives in shape optimization*. Interaction of Mechanics and Mathematics. Springer-Verlag, Berlin, Heidelberg, 2013.

- [76] A. A. Novotny, J. Sokołowski, and E. A. de Souza Neto. Topological sensitivity analysis of a multi-scale constitutive model considering a cracked microstructure. *Mathematical Methods in the Applied Sciences*, 33(5):676–686, 2010.
- [77] M. Otomori, T. Yamada, K. Izui, and S. Nishiwaki. Matlab code for a level set-based topology optimization method using a reaction diffusion equation. *Structural and Multidisciplinary Optimization*, 51(5):1159–1172, 2015.
- [78] J. T. Pereira, E. A. Fancello, and C. S. Barcellos. Topology optimization of continuum structures with material failure constraints. *Structural and Multidisciplinary Optimization*, 26(1–2):50–66, 2004.
- [79] P. Plotnikov and J. Sokołowski. *Compressible Navier-Stokes Equations. Theory and shape optimization*. Springer-Verlag, Basel, 2012.
- [80] L. F. N. Sá, R. C. R. Amigo, A. A. Novotny, and E. C. N. Silva. Topological derivatives applied to fluid flow channel design optimization problems. *Structural and Multidisciplinary Optimization*, 54(2):249–264, 2016.
- [81] B. Samet, S. Amstutz, and M. Masmoudi. The topological asymptotic for the Helmholtz equation. *SIAM Journal on Control and Optimization*, 42(5):1523–1544, 2003.
- [82] E. Sanchez-Palencia. *Non-homogeneous media and vibration theory*, volume 127 of *Lecture Notes in Physics*. Springer-Verlag, Berlin, 1980.
- [83] O. Sigmund. On the design of compliant mechanisms using topology optimization. *Mechanics of Structures and Machines: An International Journal*, 25(4):493–524, 1997.
- [84] J. Sokołowski and A. Żochowski. On the topological derivative in shape optimization. *SIAM Journal on Control and Optimization*, 37(4):1251–1272, 1999.
- [85] J. Sokołowski and A. Żochowski. Topological derivatives of shape functionals for elasticity systems. *Mechanics of Structures and Machines*, 29(3):333–351, 2001.
- [86] R. Tokmashev, A. Tixier, and B. Guzina. Experimental validation of the topological sensitivity approach to elastic-wave imaging. *Inverse Problems*, 29:125005, 2013.
- [87] A. J. Torii, A. A. Novotny, and R. B. Santos. Robust compliance topology optimization based on the topological derivative concept. *International Journal for Numerical Methods in Engineering*, 106(11):889–903, 2016.
- [88] J. Tu, K. K. Choi, and Y. H. Park. A new study on reliability-based design optimization. *ASME Journal of Mechanical Design*, 121(4):557–564, 1999.
- [89] I. Turevsky, S. H. Gopalakrishnan, and K. Suresh. An efficient numerical method for computing the topological sensitivity of arbitrary-shaped features in plate bending. *International Journal for Numerical Methods in Engineering*, 79(13):1683–1702, 2009.
- [90] N. Van Goethem and A. A. Novotny. Crack nucleation sensitivity analysis. *Mathematical Methods in the Applied Sciences*, 33(16):1978–1994, 2010.
- [91] M. Xavier, E. A. Fancello, J. M. C. Farias, N. Van Goethem, and A. A. Novotny. Topological derivative-based fracture modelling in brittle materials: A phenomenological approach. *Engineering Fracture Mechanics*, 179:13–27, 2017.
- [92] J. Zhao and C. Wang. Robust topology optimization under loading uncertainty based on linear elastic theory and orthogonal diagonalization of symmetric matrices. *Computer Methods in Applied Mechanics and Engineering*, 273:204–218, 2014.

(A.A. Novotny) LABORATÓRIO NACIONAL DE COMPUTAÇÃO CIENTÍFICA LNCC/MCT, COORDENAÇÃO DE MATEMÁTICA APLICADA E COMPUTACIONAL, AV. GETÚLIO VARGAS 333, 25651-075 PETRÓPOLIS - RJ, BRASIL  
*E-mail address:* novotny@lncc.br

(J. Sokołowski) INSTITUT ÉLIE CARTAN, UMR 7502 LABORATOIRE DE MATHÉMATIQUES, UNIVERSITÉ DE LORRAINE, NANCY 1, B.P. 239,54506 VANDOEUVRE LÈS NANCY CEDEX, FRANCE  
*E-mail address:* Jan.Sokolowski@univ-lorraine.fr

(A. Żochowski) SYSTEMS RESEARCH INSTITUTE OF THE POLISH ACADEMY OF SCIENCES, UL. NEWELSKA 6, 01-447 WARSZAWA, POLAND  
*E-mail address:* Antoni.Zochowski@ibspan.waw.pl